# **Contents**

Prefa	Introduction Preface				
Intr					
1	Crit	ical Phenomena	13		
	1.1	Critical phenomena in magnets  1.1.1 Critical exponents  1.1.2 Models of magnetism	14		
	1.2	Ising model and liquid/gas critical point: lattice gas model  1.2.1 Antiferromagnetic version of the lattice gas			
	1.3	Exact solution of the 1d Ising model  1.3.1 Spin-spin correlation function.  1.3.2 Spontaneous magnetization  1.3.3 Spin susceptibility.  1.3.4 Ising antiferromagnet in 1d.  1.3.5 Landau's argument for no phase transition in 1d.	22 23 23 24		
	1.4	2d Ising model1.4.1 Peierls argument1.4.2 Duality theorem for 2d Ising model1.4.3 Transfer matrix solution for the 2d Ising model	27 28		
	1.5	The coarse-grained Landau-Ginzburg partition function.  1.5.1 Mean field theory			
	1.6	First order phase transitions  1.6.1 First and second order phase transitions	45		

vii

		3.7.1 Statistical mechanics of the classical ordered phase	152
		3.7.2 Generalization to a finite magnetic field	162
		3.7.3 Correlation length critical exponent	162
		3.7.4 Renormalization group flows near $d = 2$	163
	3.8	Renormalization group for quantum rotors at finite temperature	165
		3.8.1 Consequences of the quantum recursion relations for $n = 3$ rotors	
		3.8.2 Crossovers for quantum rotors at $d = 2$	170
	3.9	Exercise	171
4	Line	ear Polymer Chains	173
	4.1	The random walking polymer	175
	4.2	Freely-jointed chain model: polymers with independently fluctuating segments	179
	4.3	Worm-like chain model: polymers with interacting segments	181
		4.3.1 Zero force partition function	
		4.3.2 Spontaneous mass generation in polymer chains	186
	4.4	Polymers with self-avoidance	189
		4.4.1 Flory's argument	190
		4.4.2 Continuum limit with self-avoidance	192
		4.4.3 Self-avoiding polymers and the $n \rightarrow 0$ limit of vector spins	193
		4.4.4 High temperature series expansion	194
	4.5	Alternative epsilon expansions for linear polymers	199
	4.6	Exercise	206
5	Stat	istical Mechanics of Freely Fluctuating Elastic Sheets	207
	5.1	Statistical mechanics of sheet polymers	209
		5.1.1 Connection with a metric tensor	
		5.1.2 Goldstone modes of the flat phase	211
		5.1.3 Analogy with superconductivity	213
		5.1.4 Simulation model	
		5.1.5 Low temperature statistical mechanics of the flat phase	215
	5.2	In-plane elasticity of flat sheet polymers	217
		5.2.1 Case I: finite momentum modes	
		5.2.2 Case II: zero momentum modes	
		5.2.3 Response of planar crystals to external forces	220
	5.3	Pure out-of-plane elasticity: "liquid" sheets (e.g., lipid bilayers)	222
	5.4	General treatment	224
		5.4.1 Integrating out the in-plane phonons	224
		5.4.2 Self-consistent theory	231

	5.5	Renormalization group treatment	232
	5.6	Overview of the statistical mechanics of atomically thin plates	235
		5.6.1 Nonlinear Föppl-von Kármán equations at $T = 0$	235
		5.6.2 Thin solid shells and structures	
		5.6.3 A more sophisticated renormalization group for thermalized membranes	239
		5.6.4 Experiments on graphene cantilevers	240
		5.6.5 Path integrals for long graphene ribbons	241
	5.7	Exercises	244
5	Ren	ormalization and Fluid Dynamics	249
	6.1	Basics of fluid mechanics	249
		6.1.1 Convective derivative	249
		6.1.2 Mass conservation	250
		6.1.3 Shear viscosity of Newtonian fluid	251
		6.1.4 Experimental facts	251
		6.1.5 Non-uniform shear stresses	253
	6.2	Navier-Stokes equations	253
		6.2.1 Pipe flow at low Reynolds number	256
		6.2.2 Flow past a sphere (dry water)	259
		6.2.3 Flow past a sphere (wet water)	261
		6.2.4 Energy transfer in Navier-Stokes equations	263
	6.3	Mesoscopic turbulence: Navier-Stokes with random stirring	265
		6.3.1 Time correlation functions	268
		6.3.2 Linear theory in terms of a Reynolds number	270
	6.4	Noisy Burgers equation	271
		6.4.1 Linear case: $\lambda = 0$	273
		6.4.2 General case: $\lambda \neq 0$	273
	6.5	Dynamical renormalization group	278
		6.5.1 Noise renormalization	
		6.5.2 Vertex renormalization	283
		6.5.3 Recursion relations	283
		6.5.4 Other nonlinear terms are irrelevant variables	285
		6.5.5 Surface growth	286
	6.6	Flocking and active matter	286
	6.7	Exercises	288
7	Арр	endices	293
	7.1	Path integral expression for the density matrix	293
	7.2	Path integral for O(3) quantum rotors	
	1.2	remainegration O(3) quantum rotors	493

© Copyright, Princeton University Press. No part of this book may be distributed, posted, or reproduced in any form by digital or mechanical means without prior written permission of the publisher.

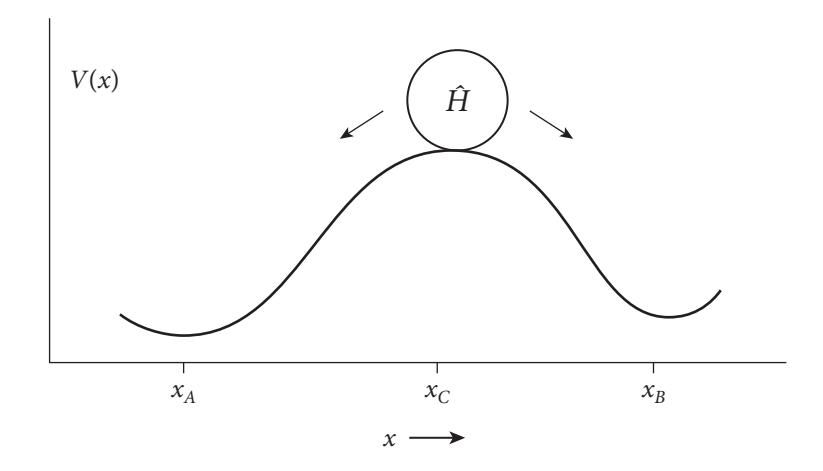
Contents ix

7.3	Mapping quantum operator correlation functions onto equal time classical path integrals	298
Bibliography		. 299
Index		305

# Introduction

The six chapters of this book that follow describe how ideas underlying the renormalization group (RG), a significant breakthrough in theoretical physics during the second half of the twentieth century, impact a broad range of areas in condensed matter physics. After reviewing Ising models, lattice gases, and critical point phenomena in Chapter 1, we show in Chapter 2 how RG methods, once migrated from particle physics to condensed matter physics, allow a deep understanding of the functional integral Landau theories that describe magnetic phase transitions of *n*-component classical spin problems, typically calculations in  $d = 4 - \epsilon$  dimensions. We then move on to Chapter 3, which covers quantum critical phenomenon, starting with a review of path integrals applied to quantum double wells and subsequently covering various quantum rotor models on a lattice, including spontaneously broken symmetries and phenomena in the vicinity of d=2 dimensions. For the problems we focus on, at both finite and zero temperature, the rotor path integrals acquire an extra dimension in imaginary time relative to their classical counterparts. Chapter 4 describes the statistical mechanics of linear polymer chains, with broad applications to biology, chemistry, and physics. When these one-dimensional assemblies of molecules, connected by strong covalent bonds, are very long and wander due to thermal fluctuations in two or three dimensions, they behave as if they are at a critical point. We cover both freely-jointed chain and worm-like chain models, and then show how renormalization group ideas can be used to understand important aspects of their behavior, such as swelling due to self-avoidance. Chapter 5 covers fluctuating sheet polymers; examples include free-standing graphene and the spectrin skeleton of red blood cells. RG methods predict a remarkable low-temperature flat phase, a rare example of a two-dimensional continuous broken symmetry that survives even at finite temperature, with remarkable scale-dependent renormalized elastic constants—for example, thermal fluctuations at room temperature can enhance the bending rigidity of graphene from its value at zero temperature by 4000-fold! The dynamics associated with the Navier-Stokes equations and simplified models of randomly stirred fluids are covered in Chapter 6 and treated with a dynamical version of the renormalization group. The properties of "active matter," driven out of equilibrium by, e.g., biologically-inspired filaments straddled by motor proteins that burn biological fuels like adenosine triphosphate (ATP), are mentioned at the very end. This Introduction is intended to provide a big-picture overview, as well as some historical context, for the contents to come. The equations presented here will be explained in detail in the subsequent chapters, so the reader should not worry if they seem unfamiliar or confusing on a first

**Figure i:** "Let  $x_C$  be the location of the maximum of V(x), i.e., the top of the hill. If the ball is released at any point  $x < x_C$  (on the left of  $x_C$ ) then the ball rolls down to the point  $x_A$  and stops. If it is released to the right of  $x_C$ , it rolls to  $x_B$  and stops." Figure and quotation are from Kenneth Wilson's seminal paper on the renormalization group for classical spin systems [5].

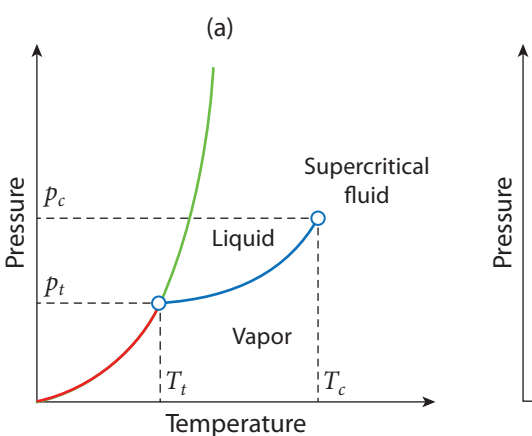


reading. Readers are encouraged to circle back and return to this chapter upon reaching the end of the book.

A modern perspective on renormalization groups owes much to Kenneth G. Wilson, who, although hired as a high energy field theorist at Cornell University during the mid-1960's, made invaluable contributions to the systematic way we think about condensed matter physics today. Wilson started publishing the seminal papers that applied RG methods to condensed matter physics problems in 1971 [5]. He postulated that in systems with phase transitions, the Hamiltonian (a function that takes many-body coordinates such as particle positions and momenta and outputs the corresponding energy) can sit like a ball poised on the top of a hill (see Figure i) and roll down the hill with motion described by a set of overdamped dynamical equations for the coupling constants. This was a striking concept at the time; physicists are used to thinking of Hamiltonians as controlling dynamics via equations of motion rather than as objects exhibiting dynamics themselves. In Wilson's picture of phase transitions, the spatial coordinates of the hill and the ball describe parameters in the Hamiltonian functional, and the time quantity is replaced by the fraction of degrees of freedom that have been coarse-grained over (see Figure i). That is, the Hamiltonian of a given system experiences dynamics as the system it describes is systematically coarse-grained in some way, and these dynamics are intimately related to the phases and phase transitions that the system exhibits. Wilson's beautiful insights were recognized by the Nobel Prize in Physics in 1982.

### Liquid/gas phase coexistence and magnetic ordering

An important problem in chemistry and physics that stimulated the breakthrough of an infrared RG (as opposed to the ultraviolet renormalization groups more common in field theories) concerns phase transitions between solids, liquids, and gases. These phases can be mapped out in a phase diagram, as in Figure iia, where the axes are temperature and pressure. In the vapor or gas phase, which



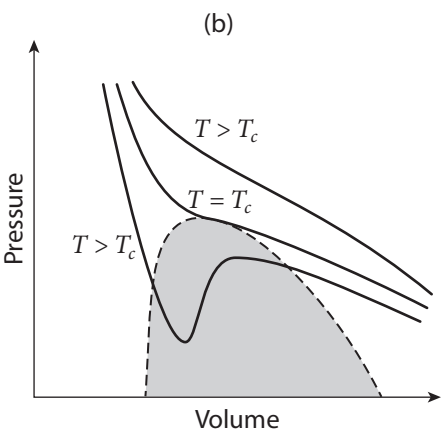


**Figure ii:** (a) Schematic of a solid-liquid-vapor phase diagram in pressure-temperature space. (b) Schematic of isotherms near liquid-gas coexistence as a function of pressure and volume at different temperatures, where  $T_c$  marks the temperature at the critical point in (a).

typically occurs at low pressure and high temperature, particles are randomly distributed and don't interact much. This phase, at least when there are short range attractive interactions between particles (as well as a repulsive hard core), is often separated by a transition line from a higher density liquid phase, where the particles remain disordered but interact much more strongly. In the solid (crystal) phase, the particles are arranged in regular repeating patterns. A natural question to ask is: What is the nature of the transitions between these different phases?

In Figure iia, the solid-vapor and liquid-vapor transitions, marked respectively by the red and blue curves, are first order phase transitions with discontinuous changes in density and entropy. The crystal-liquid transition, marked by the green line, is more subtle. A crystal has crystallographic axes, which dictate how it and its diffraction spots are oriented relative to a laboratory frame, and sets of regularly spaced Bragg planes of atoms, each of which behave like a diffraction grating. Relative to the liquid, the crystal breaks both orientational and translational symmetry. Thus, the first order green transition line separating liquid and crystalline phases never terminates (unlike the blue first order transition line between gas and liquid), as one cannot gradually abolish a pair of broken symmetries. Although not shown in Figure ii, the two broken symmetries of a crystal can sometimes be broken sequentially as a material is cooled, as in the nematic liquid crystals of oriented rod-shaped molecules. This phase is crucial for liquid crystal display devices and has a broken rotational symmetry (the molecules choose an alignment direction), but no broken translation symmetry. A crystalline phase can still exist, but only at an even lower temperature. There is an analogous fourth, hexatic liquid phase of matter, which flows freely but has the extended six-fold bond orientational order of a triangular lattice crystal and arises in layered or two-dimensional systems, even with isotropic particles. Solid, liquid and gas phases of point-like particles can simultaneously coexist at a special place on the phase diagram of Figure iia, the triple point  $(T_t, p_t)$ . (The atmospheric pressure on the surface of Mars is below the triple point of water, so don't go looking for liquid water on the Martian surface! Only ice and vapor phases of water are possible there at the present time.)

As shown in Figure iia, the liquid-gas line of coexisting phases terminates at a special critical point given by  $(T_c, p_c)$ . The critical point is itself a set of measure zero in the phase diagram, but its influence can extend far from the point itself. To illustrate this fact, imagine varying the volume and measuring the pressure at a variety of fixed temperatures to explore different features of the phase diagram. We can then plot the pressure-volume isotherms, as shown in Figure iib. At temperatures below the critical point temperature  $T_c$ , there is a vapor-liquid coexistence region, as is apparent from the Van der Waals loops in the pressure-volume isotherms. These loops are unphysical, and an equal-area Van der Waals construction is required to replace this portion of these curves by horizontal tie lines, across which liquid and vapor phases coexist with different volumes and hence different densities if the particle number is fixed [6]. As one approaches  $T_c$  from below, the distinction between liquid and gas vanishes continuously. Above  $T_c$ , each isotherm decreases monotonically with increasing volume. Something remarkable also happens as one approaches the critical point from above. As  $T \to T_c^+$ , the slope of the isotherm lines goes to zero, which means that the isothermal compressibility  $\kappa_T = -\frac{1}{V} \left(\frac{\partial V}{\partial p}\right)_T$  diverges to infinity. The isothermal compressibility is just one of many singular response functions we will encounter in this book. Its divergence already signals that remarkable phenomena happen near a critical point. As we shall see, exactly at the critical point, there are fluctuations in density (or in some other measure of order) at all scales up to the system size. This phenomenon is called critical opalescence, where initially transparent fluids become milky white and scatter light at many different wavelengths. As mentioned, below the critical point (down the blue line of vapor-liquid coexistence in Figure iia), such systems phase-separate into distinct liquid and gas phases. Phase diagrams with solid, liquid, and gas phases, including a special liquid-gas critical point with a diverging correlation length, arise for many different substances composed of molecules and atoms (e.g., methane, argon, xenon, water, toluene, acetone...). Although the critical point is typically a set of measure zero, its influence can be felt over a significant portion of the phase diagram.

Remarkably, a simple model of interacting spins in ferromagnets, important for magnetic phase transitions, can also capture phenomenon with very similar features to the gas-liquid phase transition. The Ising model describes a system of spins that can either point up or down. (We will study this model in detail in Chapter 1.) On letting  $\sigma_i = \pm 1$  denote the orientation of the *i*-th spin, the Ising Hamiltonian is given by

$$\mathcal{H}_{I} = -J \sum_{\langle ij \rangle} \sigma_{i} \sigma_{j} - h \sum_{j} \sigma_{j}, \quad \sigma_{j} = \pm 1$$
 (i)

where the exchange coupling J > 0 controls the strength of alignment between neighboring spins, and h is an external magnetic field coupled to each individual spin. The macroscopic magnetization of these spins is the average of the orientations of the individual spins  $M = \langle \sigma_i \rangle$ , where the brackets indicate a statistical mechanical average.

To draw an analogy between the Ising model of magnetic spins and the liquid-gas phase transition, imagine that the particles in the latter system sit on a lattice rather than in continuous space. At each site, a down spin corresponds to the absence of a particle, while an up spin corresponds to the presence of a particle. The external magnetic field h corresponds to the chemical potential that controls the total number of particles on the lattice (the chemical potential is another parameter, besides temperature and pressure, that one can tune to move around with in a solid-liquid-gas phase diagram). In Chapter 1, we'll see that, like the liquid-gas portion of the phase diagram in Figure iia, the simple Ising problem also has a line of discontinuous phase transitions between two distinct ferromagnetic phases (mostly up spins or mostly down spins) that terminates at a critical point, called the Curie temperature  $T_c$ . In fact, computer simulations of the Ising model in thermodynamic equilibrium reveal that the system exhibits fluctuations on all spatial scales near  $T_c$ , accompanied by a diverging correlation length, similar to a liquid-gas critical point, which we will explore in various ways in Chapters 1 and 2.

When the Ising model coupling J in Eq. i is negative, this Hamiltonian describes some aspects of the behavior of brass, a common alloy of copper and zinc. The phase diagram as a function of composition and temperature (with the pressure fixed) is shown in Figure iii. Brass has a rich variety of phases, such as  $\alpha, \beta, \beta'$ , and  $\gamma$ , characterized by different lattice structures for the positions of the zinc and copper atoms, which depend on both temperature and their relative proportions. Although Cu and Zn form a liquid binary mixture at high temperature, brass crystallizes and exhibits a two-phase region at low temperatures, where it spontaneously separates into face-centered-cubic  $\alpha$  crystals and y crystals. Unlike for the liquid-gas system and the Ising model, the phase diagram of brass has a *line* (rather than a point) of second-order phase transitions separating the two body-centered-cubic (bcc)  $\beta$  and  $\beta'$  phases, with the same lattice structure. Above the transition temperature, the zinc and copper atoms in this alloy randomly occupy the sites of the two simple cubic sublattices of this bcc lattice. Below the transition temperature, copper mostly occupies one sublattice and zinc mostly occupies the other sublattice. If we identify copper atoms with up-spins and zinc atoms with down-spins, we can map this system onto an Ising antiferromagnet, which exhibits a line of second-order phase transitions

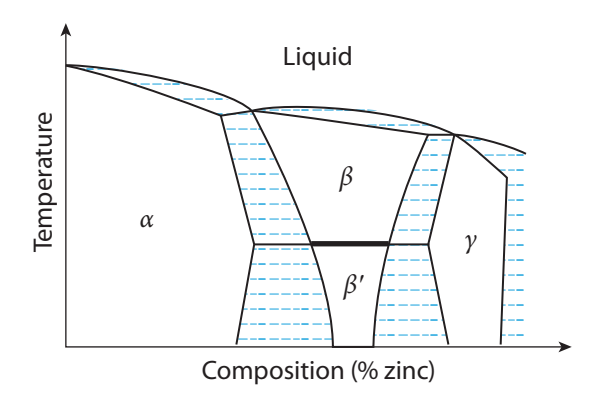


**Figure iii:** A schematic of the phase diagram of brass, an alloy of copper and zinc, in the plane of temperature and zinc weight fraction. There is a *line* of second order phase transitions, roughly at a constant temperature, separating two distinct structural phases  $\beta$  and  $\beta'$ . The horizontal dashed lines span regions of two-phase coexistance.

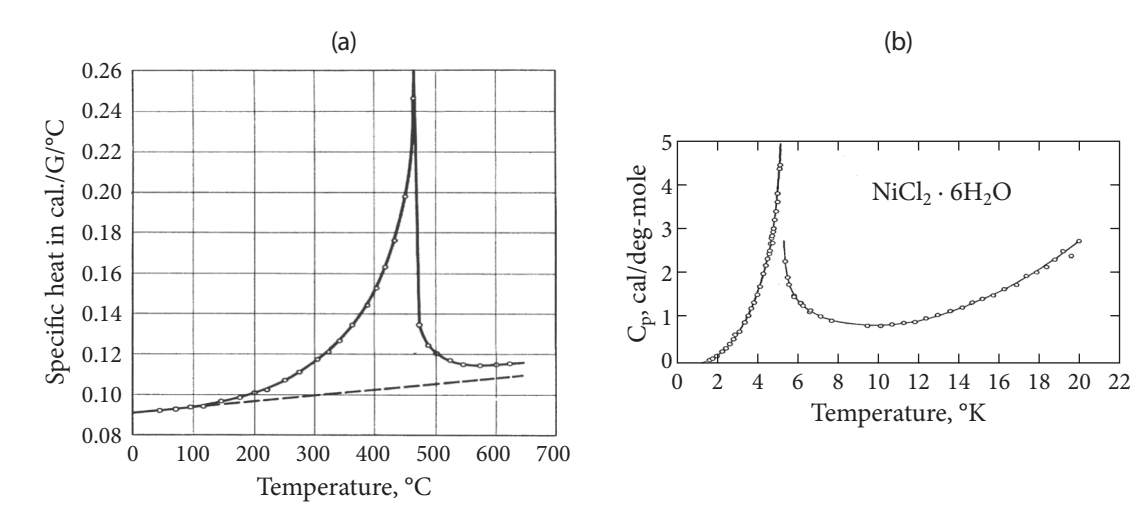


**Figure iv:** Specific heat curves as a function of temperature for both (a)  $\beta$ -brass and (b) zerofield Ising antiferromagnets (e.g. NiCl<sub>2</sub>· 6H<sub>2</sub>O) exhibit the same power-law divergence upon approaching the critical points of these systems. Figure adapted from Refs. [7, 8].

separating the antiferromagnetic phase and the paramagnetic phase in the h-Tphase diagram; see Chapter 2 for details.

On measuring the specific heat of  $\beta$ -brass at fixed composition while the system approaches the critical line segment in the phase diagram in Figure iii, one finds that the specific heat rises to a singularity at the critical line. Similarly, the zero-field specific heat of an Ising antiferromagnet also diverges as one approaches the Curie transition temperature  $T_c$ . In both cases, the specific heat curves near the respective critical points can be fit to a power law singularity with the same critical exponent (see Figure iv)! This shared behavior between antiferromagnets and  $\beta$ -brass is an example of universality: Quite different physical systems can share similar properties near critical points, regardless of their microscopic details. Chapters 1 and 2 will explore the question, where do these singularities come from and can we understand the apparently universal behaviors shared by these different systems?

An important message to take away from this book is that the renormalization group maps hard problems onto easier ones. Ising models near the critical point given by the dimensionless ratio  $K_c = J/k_BT_c$  and liquid-gas systems on the verge of critical opalescence are hard to understand because they exhibit fluctuations at all spatial scales. In 1966, Leo Kadanoff [10] envisioned dividing a system of spins (interacting with dimensionless coupling constant  $K = J/k_BT$ ) into blocks and coarse-graining within each block by replacing all the spins in each block with a (super-)spin (see Figure v). These super-spins then interact with each other via a new interaction constant K'. Interestingly, the Hamiltonian under an approximate coarse-graining procedure has a fixed point, i.e., a position at the top of a hill in K-space (denoted by x in Figure i), where the coupling constants are invariant to coarse-graining. If the Hamiltonian (ball) is to the left of this fixed point, then it will roll to the left (high temperatures); if the Hamiltonain (ball) is to the right of this fixed point, then it will roll to the right (low temperatures). The crest of the hill corresponds to  $T_c$  itself. We can therefore map

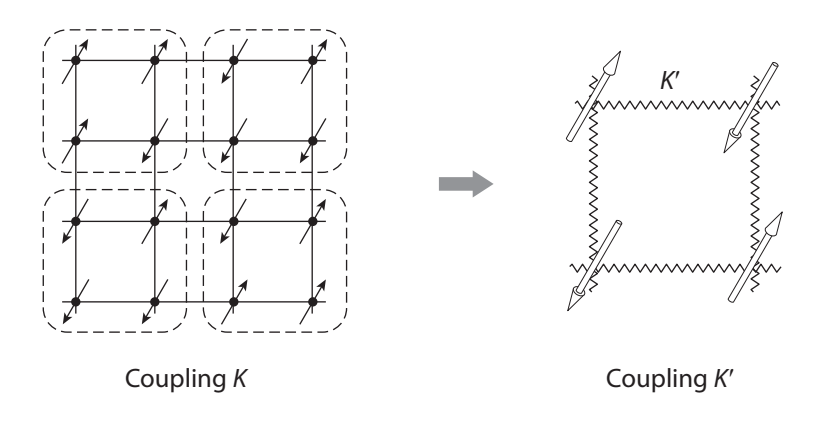


**Figure v:** Leo Kadanoff's block spin transformation for an Ising model on a square lattice. Configurations of block spins, interacting with a new coupling constant K', can be obtained from the original spins by a simple "majority rule": the new block spin is up if the original block has 3 or 4 up spins, and down if the original block has 3 or 4 down spins. An up or down block spin is chosen randomly if there is a tie within a block. Figure adapted from Ref. [9].

the Hamiltonian of the hard problem (i.e., an Ising system near the critical point  $K \approx K_c$ ) to either a low-temperature problem or a high-temperature problem, where all spins are, respectively, either mostly aligned or mostly uncorrelated, allowing for the use of various approximation schemes.

#### Quantum critical phenomena

The Hamiltonian of a non-relativistic many-particle system typically has a quadratic kinetic energy from the momentum degrees of freedom, as well as potential energy from the interactions between the individual constituents. In other words, we have a Hamiltonian of the form

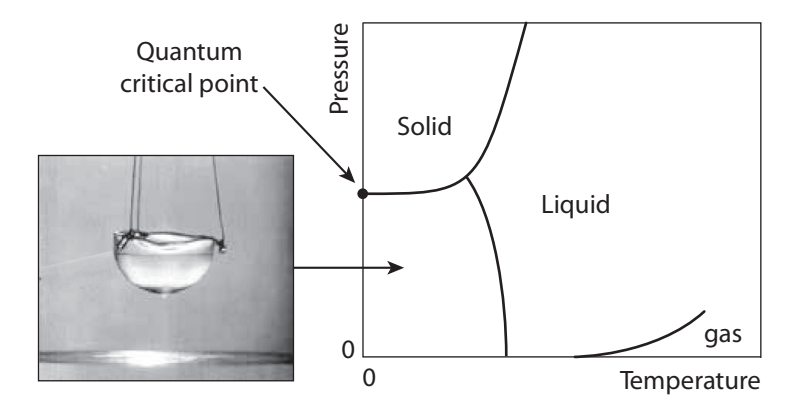
$$\mathcal{H} = \sum_{i} \frac{|\vec{p}_i|^2}{2m} + \sum_{i \neq j} \phi(|\vec{q}_i - \vec{q}_j|)$$
 (ii)

where  $\vec{p}_i$  and  $\vec{q}_i$  are the momentum and position of the *i*-th particle, respectively, and  $\phi(|\vec{q}_i - \vec{q}_j|)$  describes a pairwise interaction potential between two particles, e.g., a hardcore repulsion at short separation distances and Van der Waals attraction at long distances, as in a Lennard-Jones pair potential. When classical physics dominates over quantum effects, such interactions give rise to the usual solid, liquid, and gas phases. However, at sufficiently low temperatures, quantum mechanics can change our perspective.

In classical statistical mechanics, one can immediately integrate out all the momentum degrees of freedom, since they appear as decoupled quadratic terms with effects that are independent of one another in Eq. ii. The Gaussian integrals associated with these kinetic degrees of freedom can be easily eliminated from the partition function, although a challenging classical statistical mechanics problem involving the potential energy still remains. However, the statistical physics is more challenging in quantum systems, because momentum and position are intertwined by the uncertainty principle. Indeed, their corresponding operators (indicated by a circumflex) don't commute,

$$[\hat{p}_i^{\alpha}, \hat{q}_i^{\beta}] = i\hbar \delta_{ij} \delta_{\alpha\beta}. \tag{iii}$$

Figure vi: Helium-4 exhibits a quantum phase transition from solid to superfluid as a function of pressure at sufficiently low temperatures. In the superfluid phase at low temperature and pressures, the bulk Helium liquid in the container at left can escape by flowing through a porous material, or by forming a thin film that flows without resistance. All phase boundaries describe first order transitions, except the line separating the high temperature liquid from the low temperature superfluid. (Adapted from video by Alfred Leitner, Liquid Helium, Superfluid (1963), available on Youtube.)



In fact, quantum zero-point motion, intimately connected with this nonzero commutator, can disrupt perfect order at very low temperatures in intriguing ways. For example, below about  $2.5^{\circ}$  K, liquid Helium 4 exhibits a new phase of matter—a superfluid—so called because it flows without resistance even in the thinnest films and through the finest capillary tubes, i.e., it has zero shear viscosity. The He<sup>4</sup> crystal becomes unstable with decreasing pressures near T=0 to the superfluid phase due to the residual quantum zero-point vibrations of the crystal lattice. This phase transition between solid and superfluid He<sup>4</sup> is a quantum first-order transition in three dimensions (see Figure vi). In this case, the first-order quantum transition is associated with a changeover between two very different many-body ground state wave functions, and involves the crossing of two competing ground state energies. Outside of two dimensions, for which a continuous transition to a quantum hexatic phase is possible [11], there are no diverging correlation lengths and no critical phenomena in a conventional sense, because the transition is first-order.

However, quantum critical phenomena near T=0 does arise in other contexts, such as quantum antiferromagnets [12, 13]. Another paradigmatic quantum problem, which we will study extensively in Chapter 3, is a lattice of interacting quantum rotors. As is well known from the study of ideal gases with structure, diatomic molecules have important vibrational modes and rotational modes in isolation. If the bonds within the molecules are very stiff, then the most important remaining descriptor of each molecule in isolation is its angular momentum. The Hamiltonian of a system of these stiff rotors on a lattice has a kinetic energy from the rotation of the molecules and a potential energy from the alignment interaction between neighboring molecules, as shown here

$$\mathcal{H}_R = \frac{Jg}{2} \sum_i \hat{L}_i^2 - J \sum_{\langle ij \rangle} \hat{n}_i \cdot \hat{n}_j, \qquad (iv)$$

where Jg and J are coupling constants parameterizing the strength of the kinetic energy and the alignment interaction, respectively, and the second term sums over nearest neighbor rotor pairs on a lattice. The  $\hat{L}_i$  and  $\hat{n}_i$  operators describe the angular momentum and the size and direction of the i-th rotor. The first kinetic energy coupling constant in Eq. iv comes from the moment of inertia

of the rod-like molecule. Given an alignment interaction coefficient J (somewhat like a Heisenberg exchange coupling coefficient for a spin system) for the potential energy of neighboring rotors, it is convenient to rewrite the kinetic energy parameter (scaling out J) as Jg, so g is a measure of the ratio of the kinetic to potential energy. Here, again, the momentum and interaction degrees of freedom of the rotors on the same site are linked by quantum mechanics, with nonzero commutators, summarized as follows (see Chapter 3 for more details),

$$\hat{L}_{\alpha} = \epsilon_{\alpha\beta\gamma} \, \hat{n}_{\beta} \hat{p}_{\gamma} \tag{v}$$

$$\left[\hat{L}_{\alpha}, \hat{L}_{\beta}\right] = i\epsilon_{\alpha\beta\gamma} \, \hbar \hat{L}_{\gamma} \tag{vi}$$

$$\left[\hat{n}_{\alpha},\hat{L}_{\beta}\right] = i\hbar\varepsilon_{\alpha\beta\gamma}\,\hat{n}_{\gamma}.\tag{vii}$$

We use the summation convention for repeated indices throughout this book.

In both two- and three-dimensional versions of this model, quantum rotors exhibit a second-order phase transition as g varies at T=0. In the limit of large Jg, the kinetic energy dominates, and the rotors minimize their ground state energy in a quantum disordered state. When quantum fluctuations are weak, however, interactions dominate and the rotors align in an ordered phase only mildly perturbed by quantum fluctuations. Away from zero temperature, this system of quantum rotors can experience important crossover phenomena, such that the quantum critical regime, much like the critical point in Figure iia, can influence response functions some distance away from the critical point in the phase diagram. Chapter 3 explores the rich physics associated with this simplified quantum phase transition problem.

### Fluctuating polymers

Polymers are all around us: Cross-linked polymers make up rubber bands. Polystyrene, when cooled down from a melt, has a tangled glass phase useful for disposable coffee cups and packing material. Polyethylene oxide (also called

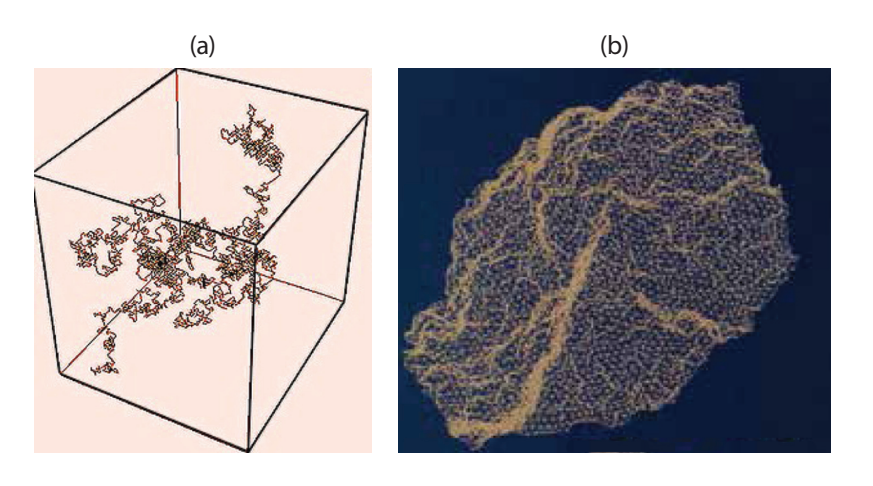


Figure vii: The effect of thermal fluctuations on the behavior of linear and sheet polymers is very different. (a) Thermal fluctuations always crumple linear polymer chains when they are sufficiently long. (b) Sheet polymers (e.g., free-standing graphene) have a wrinkled flat phase, with long range order in the normal vectors even at finite temperatures. Figure adapted from Refs. [14, 15].

polyethylene glycol) is a turbulence damper, a dilute concentration of floppy molecular chains that help the water slide through the hose of a firefighter and shoot up higher than unadulterated water. Chapters 4 and 5 are devoted to the study of chain and sheet polymers, and the insight renormalization group methods can provide.

A chain polymer wandering about in a solution at finite temperature is analogous to a classical spin chain, with the spins being the tangent vectors pointing along the backbone of the polymer. The aligning of these spins then corresponds to the polymer being stretched out along a single direction. As shown in Chapter 4, however, linear polymers are almost always crumpled up, with no long-range order in the orientation of their backbones. Nevertheless, when these polymers are very long, they behave as if they are at a critical point, with nontrivial critical exponents describing their conformations in the presence of self-avoiding interactions. Remarkably, this problem of polymers with self-avoidance is intimately connected with the physics of classical n-component spins in d-dimensions in the limit  $n \to 0$ , as we will discuss.

In the late 1980's and early 1990's, the statistical mechanics of chain polymers was extended to that of sheet polymers, that is, fishnet-like structures of covalently bonded monomers in two dimensions. Unlike linear polymers, sheet polymers do exhibit a low-temperature flat phase: although these itethered surfaces are corrugated, the normal vectors of the sheet all point on average in the same direction. The long-range order exhibited by these normal vectors thus evades the well-known Mermin-Wagner-Hohenberg theorem, which states that thermal fluctuations will almost always destroy long-range order in systems in two dimensions or less. Elastic parameters such as the bending rigidity and shear modulus are not in fact constants, but instead become strongly scale-dependent. There are a number of experiments studying sheet polymers with stiff covalent bonds, from observation of the rag (crumpled) phase of MoS<sub>2</sub> in 1979 [16], studies of crumpled graphite oxide in 1991 [17], and, more recently, elegant probes of the bending rigidity of graphene ribbons in the flat phase in 2015 [18]. Using the results of Chapter 5, one can show that an atomically thin sheet of graphene 10 microns across (i.e., an aspect ratio of about 40,000) has a bending rigidity that is roughly 4000 times stronger than that predicted by quantam density functional theory, simply due to thermal fluctuations. If the graphene sheet were instead 50 microns across, then its bending rigidity would be approximately 20,000 times stronger than that predicted by density functional theory for unwrinkled graphene at T = 0.

#### Fluid dynamics and dynamical renormalization groups

Fluid dynamics is a rich, challenging field with many outstanding challenges, a prime example of which is turbulence, described by a system of nonlinear partial differential equations, when a dimensionless coupling constant called the Reynolds number is very large. Chapter 6 begins with an introduction to basic fluid mechanics and leads eventually to a *dynamical* renormalization group, allowing us to compute correlations across both space and time for a

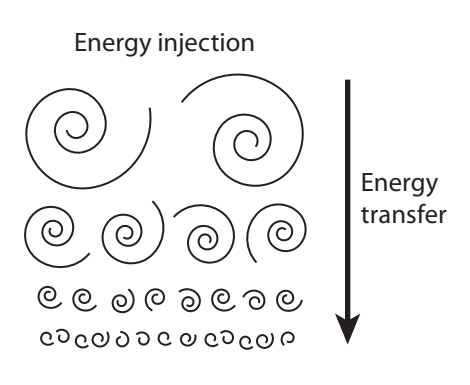




Figure viii: Left: Schematic of the Kolmogorov energy cascade in the context of turbulence, arising from nonlinearities in the Navier-Stokes equations. Right: Flocks of starlings, schools of fish, and swarms of bacteria can be described by hydrodynamical theories similar to the Navier-Stokes equations, some of which can be treated using renormalization group methods. Starling image provided by Irene Giardina. See also Ref. [19].

simplified model in the presence of advective nonlinearities, where the velocity field is purely longitudinal and subject to random stirring over many different wavelengths. The nonlinear equations believed to embody the behavior of simple, incompressible fluids were written down by Navier and Stokes in 1841 (shown here in the absence of stirring for simplicity),

$$\partial_t \vec{u} + (\vec{u} \cdot \vec{\nabla}) \vec{u} = -\frac{1}{\rho_0} \vec{\nabla} p + \nu \nabla^2 \vec{u}$$
 (viii)

$$\vec{\nabla} \cdot \vec{u} = 0, \tag{ix}$$

where  $\vec{u}(\vec{x},t)$  and  $p(\vec{r},t)$  are the velocity and pressure fields of the fluid,  $\rho_0$  is the fluid density, and  $\nu$  is its shear viscosity. To this day, these equations are not completely understood (see the fluid mechanics chapters in the Feynman Lectures in Physics), especially in the presence of the strong advective nonlinearity  $(\vec{u} \cdot \vec{\nabla})\vec{u}$ , which produces mode couplings between modes of velocity fields at different wavelengths. It is known qualitatively that large eddies excited by macroscopie stirring transfer their energy into smaller eddies, which then transfer their energy to even smaller eddies and so on. This is called the energy cascade. This energy cascade generates many distinct time and length scales for velocity excitations, somewhat reminiscent of a system at its critical point (see Figure viiia). On non-dimensionalizing Eq. viii, the coupling constant in front of the adrective nonlinearity becomes a parameter called the Reynolds number,

$$Re = \frac{L_0 u_0}{v},$$
 (x)

where  $L_0$  is the characteristic macroscopic system size (e.g., size of a stirred coffee cup),  $u_0$  is the characteristic fluid velocity magnitude at that length scale, and  $\nu$  is the kinematic viscosity that dissipates the energy. The idea is that kinetic energy is typically injected at large scales by stirring at large length scales. The large whirls then cascade down to whirls of smaller length scales until the length scales are so small that the derivative terms involving the Laplacian and the shear viscosity become large enough to produce dissipation. The Reynolds number (or nonlinear coupling strength) of cigarette smoke in the air is on the order of 100 to 1000, while the Reynolds number of oceanic flows excited by the wind-wave

coupling can easily be  $10^8$  to  $10^9$ . It's evident that we cannot use perturbation theory to treat such large nonlinearities! As discussed in Chapter 6, renormalization group methods can help, at least for a simplified model system. Our final chapter concludes with a brief review of recent ideas in the field of active matter, such as spontaneous continuous symmetry breaking in simplified flocking models of bacteria, birds, and fish. Here renormalization group methods predict that simplified hydrodynamic models of non-equilibrium active matter can support long-range order of a vector velocity order parameter, even in two dimensions.

© Copyright, Princeton University Press. No part of this book may be distributed, posted, or reproduced in any form by digital or mechanical means without prior written permission of the publisher.

# Index

adenosine triphosphate (ATP), 1, 265, 286 alternative epsilon expansions, 199–206 antiferromagnetic version of lattice gas, 21–22 Aronovitz, J. A., 239

bacterial turbulence, 265–271; flocking and active matter, 286–288; linear theory in terms of Reynolds number, 270–271; time correlation functions, 268–270 Berezinski-Kosterlitz-Thouless transition, 157 biological polymers, 173–174 Burgers equation. See noisy Burgers equation

classical ordered phase, 152–162
Clausius-Clapeyron equation, 45
condensed matter physics, 1–2, 75, 150, 175
continuum limit, 66, 69–70, 143, 152, 182–183, 247; with self-avoidance, 192–193
convective derivative, 249–250
correction to scaling, 100
correlation functions: Fourier analysis and, 64–66; generation function for higher order, 69–70; magnetic susceptibility and, 64–70; magnetization, 66–69; mapping quantum operator, onto equal time classical path integrals, 298

correlation length, 8, 15, 16, 83–84, 110, 113; classical spin system, 146; connection with 1d Ising model at low temperatures, 126–129; critical exponent, 56, 59, 69, 96, 162–163; divergence at zero temperature, 25, 115; finite temperature rotors, 151, 156; first order phase transitions, 43, 50; Ginzburg criterion, 57; lattice spacing and, 35; mean field theory and, 53; measured in units of coarse-grained lattice constant, 81; phase diagrams, 4; scaling relation for, 94–95, 100; spherical inclusion effect, 55; spontaneous magnetization, 23; susceptibility, 84–85, 106

critical exponents, 14–17; correlation length, 162–163; Ginzburg criterion and, 57–58;

in renormalization group with interactions, 98–100 critical opalescence, 4, 6 critical phenomena: beyond mean field theory, 53–58; coarse-grained Landau-Ginzburg partition function, 34–43; critical exponents, 14–17; exact solution of the 1d Ising model, 22–26; first order phase transitions, 43–53; Ising model and liquid/gas critical point, 19–22; in magnets, 13–18; models of magnetism, 17–18; quantum (*see* quantum critical phenomena); 2d Ising model, 26–34

dangerous irrelevant variables, 106–109
de Gennes, P. G., 51, 199
density matrix, 118–120, 141, 143; path integral
expression for, 293–295
dry water, 259–261
duality theorem for 2d Ising model, 28–31
dynamic renormalization groups, 10–12,
278–286; noise renormalization, 282;
other nonlinear terms as irrelevant
variables, 285–286; recursion relations,
283–285; surface growth, 286; vertex
renormalization, 283

Edwards, Sam, 192 elasticity, 230–233, 241; analogy with superconductivity, 212–214; flat sheet polymers, in-plane, 217–222; pure out-of-plane, 222–224; simulation model, 214–217 energy transfer in Navier-Stokes equations,

263-265

finite temperature rotors, 151–165; correlation length critical exponent, 162–163; generalization to finite magnetic field, 162; renormalization group flows near d=2, 163–165; renormalization group for quantum rotors at finite temperature, 165–171; statistical mechanics of classical ordered phase, 152–162

first order phase transitions, 43–45; mean field theory and Ising model, 45–50; in nematic liquid crystals, 50–53
Fisher, Michael, 185
flat sheet polymers. See sheet polymers flexural phonons, 208, 211, 212, 235–236 flocking and active matter, 286–288
Flory, Paul, 189
Flory's argument, 190–192
flow at low Reynolds number, 256–259 flow past a sphere: dry water, 259–261; wet water, 261–262

fluctuating polymers, 9–10, 179–181, 207–209; analogy with superconductivity, 212; connection with metric tensor, 210–211; dynamical renormalization group, 278–286; general treatment, 224–232; Goldstone modes of flat phase, 211–212; in-plane elasticity of flat sheet polymers, 217–222; low temperature statistical mechanics of flat phase, 215–217; overview of statistical mechanics of atomically thin pates, 235–244; pure out-of-plane elasticity, 222–224; simulation model, 214–215; statistical mechanics of sheet polymers and, 209–217

fluid mechanics, 10–12; basics of, 249–253; convective derivative, 249–250; experimental facts, 251–252; flocking and active matter, 286–288; mass conservation, 250–251; mesoscopic turbulence, 265–271; Navier-Stokes equations, 249, 253–265; noisy Burgers equation, 271–278; non-uniform shear stresses, 253; shear viscosity of Newtonian fluid, 251

Föppl-von Kármán equations, 235–238
Föppl-von Kármán number, 230–231, 235, 237
Fourier analysis, 64–66; magnetization
correlation function, 66–69
fractal dimensions, 202–203, 206
freely-jointed chain model of polymers,
179–181

- functional integrals, 16, 35, 37, 53-54, 63, 65, 110, 120-121, 148, 154, 179, 187, 204, 209-210; generalized Landau, 61; Landau-Ginzburg free energy, 45; perturbation theory, 71; quantum spin models, 42-43; superfluid Helium 4, 41
- Gaussian model: generation for higher order correlations, 69-70; noisy Burgers equation, 272-278; renormalization group for, 80-85
- generating function for higher order correlations, 69-70

Gibbs-Duham relation, 43

Gibbs free energy, 43-44

Ginzburg criterion, 57-58

Ginzburg-Landau theory of superconductivity, 212-214

Goldstone modes of flat phase, 211-212 graphene, 1, 10; cantilevers, 175, 240-241; electrons, 207; fluctuating sheets, 230-231, 233, 235, 237; FvK equations, 238; ribbons, path integrals for, 241-244; simulation model, 214-215

graphical rules, calculation of magnetization correlations, 74-79

Hamiltonian models, 2, 5, 7 Heisenberg models, 17-18, 63 Heisenberg spins, 175, 185, 215, 223; magnetization, 179-180; partition function of quantum, 42; realization of quantum rotors from quantum, 137-139,

high-temperature series expansion, 194-199; partition function, 194-197; spin-spin correlation function, 197-199

Hohenberg-Mermin-Wagner theorem, 156, 158, 175, 184, 216, 234; Goldstone modes invoked by, 209; Heisenberg spins and, 223; low temperature flat phase violating, 205; renormalization group for quantum rotors at finite temperature, 166

in-plane elasticity of flat sheet polymers, 217-222

in-plane phonons, 224-231, 239 interactions, renormalization group with, 85-102; corrections to scaling, 100; other critical exponents in, 98-100; other irrelevant variables, 100-102

irrelevant variables, 89, 100-102, 106-109, 285-286, 288

Ising models, 4-5, 19-20; antiferromagnet in 1d, 24;antiferromagnetic version of lattice gas, 21-22; compared to worm-like chain model, 185; duality theorem for 2d, 28-31; exact solution of 1d, 22-26; Landau's argument for no phase transition in 1d, 24-26; mean field

theory and first order transitions in, 45-50; Peierls argument, 27-28; spin-spin correlation function, 22-23; spin susceptibility, 23-24; spontaneous magnetization, 23; transfer matrix and the double-well quantum oscillator, 124-129; transfer matrix solution for 2d. 31-34; 2d, 26-34

isothermal compressibility, 4, 13, 43

Kadanoff, Leo, 6 Kardar-Parisi-Zhang (KPZ) equation, 272 Kramers, Hendrik, 28

Landau-Ginzburg partition function, coarse-grained, 34-43; mean field theory, 37-41; other functional integrals, 41-43; quantum spin models, 42-43; Superfluid Helium 4, 41

Landau's argument for no phase transition in 1d, 24-26

lattice constant, coarse-grained, 81; correlation length, 83-84; wave vector-dependent susceptibility, 84-85

lattice gas model, 19-22, 115, 116; antiferromagnetic version of, 21-22

linear polymer chains, 173-175; alternative epsilon expansions for, 199-206; freely-jointed chain model, 179-181; random walking polymer, 175-179; with self-avoidance, 189-199; zero force partition function, 185-189

linear theory in terms of Reynolds number,

lipid bilayer, 207, 217, 222-224, 246-247 liquid crystals, 3; first order transitions in nematic, 50-51

liquid/gas phase coexistence, 2-7 liquid sheets, 222-224

London, Fritz, 212

London, Heinz, 212

low temperature, 1, 5-7, 96, 106, 110, 123-124, 145, 181-183, 223, 243; analogy with superconductivity, 212-213; connection with the 1d Ising model at, 126-129; correlation length at, 23, 164-165; droplet energy, 49, 50; finite temperature rotors, 151; flat phase statistical mechanics, 215-217; Ising partition function, 30-31; Landau's argument for no phase transition in 1d, 24-25; 1d classical Ising model, 125; perturbation theory, 238-239; quantum critical phenomena, 7-8; sheet polymers flat phase, 10; spin susceptibility behavior at, 24; statistical mechanics of classical ordered phase, 152-158; superfluid transition in, 34; zero-field renormalization, 163-164

Lubensky, T. C., 239

magnetic ordering, 2-7 magnetic susceptibility, 13-16, 52, 58, 64 magnetization correlation function, 66-69 magnets, critical phenomena in, 13-18 mass conservation, 250-251

mean field theory: coarse-grained Landau-Ginzburg partition function, 37-41; estimating behavior of correlation length and, 53-56; and first order transitions in Ising models, 45-50; Ginzburg criterion and, 57-58

membrane, 206-209, 231-232; experiments on graphene cantilevers, 241; Goldstone modes of flat phase, 211, 214; more sophisticated renormalization group for thermalized, 239-240; nonlifnear Föppl and von Kármán equations at T = 0, 235–236; normal-normal correlations in liquid, 246-247; pure out-of-plane elasticity, 222-224, 226; thin solid shells and structures, 238-239

Mermin-Wagner-Hohenberg theorem, 10 mesoscopic turbulence, 265-271; linear theory in terms of Reynolds number, 270-271; time correlation functions, 268-270

metric tensor, 210-211 momentum degrees of freedom, 7-8 Monte Carlo simulations of path integrals, 121-122

Moore's Law, 241

Navier-Stokes equations, 249, 253-265; energy transfer in, 263-265; flow past a sphere (dry water), 259-261; flow past a sphere (wet water), 261-262; pipe flow at low Reynolds number, 256-259; with random string, 265-271

nematic liquid crystals, first order transitions in, 3,50-53

noise renormalization, 282

noisy Burgers equation, 271-278; general case, 273-278; linear case, 273; noise renormalization, 282; other nonlinear terms as irrelevant variables, 285-286; recursion relations, 283-285; surface growth, 286; vertex renormalization,

nonlinear Föppl-von Kármán equations at T = 0.235 - 238non-uniform shear stresses, 253

O(2) quantum rotors, two-component, 129-132 O(3) quantum rotors: path integral for, 295-298; three-component, 132-139

1d Ising model: exact solution of, 22-26; Ising antiferromagnet in, 24; Landau's argument for no phase transition in, 24-26; at low temperatures, 126-129; transfer matrix and the double-well quantum oscillator, 124-129

out-of-plane elasticity of polymer sheets, 222–224

out-of-plane phonons. See flexural phonons

particle in a quantum double well, 122–129; 1d classical Ising chain, 124–129

partition function, high temperature series expansion, 194–197

path integrals: expression for density matrix, 293–295; for long graphene ribbons, 241–244; mapping quantum operator correlation functions onto equal time classical, 298; Monte Carlo simulations of, 121–122; for O(3) quantum rotors, 295–298; and quantum statistical mechanics, 117–121; for rigid rotors, 139–147

Peierls argument, 27-28

perturbation theory, 71–80; fixing, 80; graphical rules, 74–79; vertex renormalization, 79 phase transitions: classical ordered, 152–162; first and second order, 43–45; first order,

first and second order, 43–45; first order, in nematic liquid crystals, 50–53; mean field theory and Ising model first order, 45–50

phonons: flexural, 208, 211, 212, 235–236; in-plane, 224–231, 239

pipe flow at low Reynolds number, 256–259 polymers: alternative epsilon expansions for linear, 199–206; biological, 173–174; flat sheet (*see* sheet polymers); fluctuating (*see* fluctuating polymers); high temperature series expansion, 194–199; with interacting segments, 181–189; linear (*see* linear polymer chains); pure out-of-plane elasticity, 222–224; solid, 173; spontaneous mass generation in, 186–189; statistical mechanics of sheet,

pure out-of-plane elasticity, 222-224

209-217

quantum critical phenomena, 7–9, 115–117; finite temperature rotors, 151–165; Monte Carlo simulations of path integrals, 121–122; particle in a quantum double well, 122–129; path integral for rigid rotors, 139–147; path integrals and quantum statistical mechanics, 117–121; quantum ordered phase, 147–150; three-component O(3) quantum rotors, 132–139; two-component O(2) quantum rotors, 129–132

quantum operators, 298 quantum ordered phase, 147–150 quantum recursion relations, 169–170 quantum rotors: consequences of quantum recursion relations for n=3, 169–170; crossovers for, at d=2, 170–171; path integral for O(3), 295–298; realization from quantum Heisenberg spins,

137–139; renormalization group for, at finite temperature, 165–171; three-component O(3), 132–139; two-component O(2), 129–132 quantum spin models, 42–43

random walking polymer, 175–179 recursion relations, 283–285

renormalization groups (RG), 1–2; correlation functions, 64–70; dangerous irrelevant variables, 106–109; direct calculation of susceptibility near four dimensions, 102–106; dynamic, 10–12, 278–286; flows near d=2, 163–165; fluid mechanics (see fluid mechanics); for the Gaussian model, 80–85; with interactions, 85–102; liquid/gas phase coexistence and magnetic ordering and, 2–7; perturbation theory, 71–80; for quantum rotors at finite temperature, 165–171; sheet polymers, 232–235; for thermalized membranes, 239–240; wavelength fluctuations, 63–64

Reynolds number: dry water, 259–261; linear theory in terms of, 270–271; pipe flow at low, 256–259; wet water, 261–262

rigid rotors, path integral for, 139-147

scaling corrections, renormalization group with interactions, 100

second order phase transitions, 43–45 self-avoidance, polymers with, 189–199; continuum limit, 192–193; Flory's argument on, 190–192; high temperature series expansion, 194–199; *n*-component spins, 193–194

self-consistent theory, sheet polymer, 231–232 shear stresses, 222; non-uniform, 253 shear viscosity, 8, 11, 35, 251, 252, 256, 282, 289

sheet polymers, 209-222; analogy with superconductivity, 212-214; connection with metric tensor, 210-211; finite momentum modes, 217-218; general treatment, 224-232; Goldstone modes of flat phase, 211-212; in-plane elasticity of flat, 217-222; integrating out the in-plane phonons, 224-231; low temperature, flat phase, 215-217; overview of statistical mechanics of atomically thin plates, 235-244; pure out-of-plane elasticity, 222-224; renormalization group treatment, 232-235; response of planar crystals to external forces, 220-222; self-consistent theory, 231-232; simulation model, 214-215; zero momentum modes, 218-220

shell, momentum, 81, 86–87 simulation, 5, 28, 31; bacteria swarms flocking, 287; beyond mean field theory, 53; Heisenberg model, 164; Monte Carlo, of path integrals, 121–122; Navier-Stokes with random stirring, 265–268; sheet polymers, 214–215; Toner-Tu model, 287 spin-spin correlation function, 22–23, 197–199 spin susceptibility, 23–24 spontaneous magnetization, 23 spontaneous mass generation in polymer chains, 186–189

statistical mechanics, 7, 10, 17, 46, 51, 67, 115–116, 173; of atomically thin plates, 235–244; of the classical ordered phase, 152–162; coarse-grained Landau-Ginzburg partition function, 34; lattice gas model, 19; low temperature, of the flat phase, 215–217; particle in a quantum double well, 122–124; path integrals and quantum, 117–118; polymers with independently fluctuating segments, 179–181, 183; of sheet polymers, 209–215

stirred fluids, 278, 285; absence of flocking, 286; in bacterial turbulence, 266; energy of, as function of time, 264; energy of, equal to kinetic energy, 269; Navier-Stokes equations of, 249, 266

superconductivity, 212–214 superfluid Helium 4, 41

surface growth, noisy Burgers equation, 286 susceptibility: coarse-grained magnetic system, 38–39; critical exponents, 15–16; dangerous irrelevant variables, 106–109; direct calculation of, near four dimensions, 102–106; Ginzburg criterion, 57; graphical rules, 75–79; magnetic, 13–14, 64–70, 98–99, 189; perturbation theory to calculate, 72; in presence of nonzero magnetic field, 129;

scaling argument for wave vector-dependent, 84–85; spin, 23–24, 193–194, 197, 199; zero field inverse, 39–40

thin plates: experiments on graphene cantilevers, 240-241; more sophisticated renormalization group for thermalized membranes, 239-240; nonlinear Föppl-von Kármán equations at T=0, 235-238; path integrals for long graphene ribbons, 241-244; thin solid shells and structures, 238-239

three-component O(3) quantum rotors, 132–139

Toner, John, 288

transfer matrix solution for 2d Ising model, 31-34

Tu, Yuhai, 288

2d Ising model, 26–34; duality theorem for, 28–31; Peierls argument, 27–28; transfer matrix solution for, 31–34 308 Index

two-component O(2) quantum rotors, 129–132 two-dimensional sheet polymers. *See* sheet polymers

vertex renormalization, 79, 283 viscosity, shear, 8, 11, 35, 251, 252, 256, 282, 289 Wainnier, Gregory, 28 wet water, 261–262 Wick's theorem, 69–70; perturbation theory and, 71–73 Wilson, Kenneth G., 2 worm-like chain model of polymers, 181–189;

spontaneous mass generation in,

186–189; zero force partition function, 185–189

XY model susceptibility below  $T_c$ , 106–109 XY rotor path integrals, 139–147

zero force partition function, 185-189